The distributions of random matrix theory have seen an explosion of interest in recent years, and have been found in various applied fields including physics, high-dimensional statistics, wireless communications, finance, etc. The Tracy-Widom distribution is one of the most important distributions in random matrix theory, and its numerical evaluation is a subject of great practical importance. One numerical method for evaluating the Tracy-Widom distribution uses the fact that the distribution can be represented as a Fredholm determinant of a certain integral operator. However, when the spectrum of the integral operator is computed by discretizing it directly, the eigenvalues are known to at most absolute precision. Remarkably, the integral operator is an example of a so-called bispectral operator, which admits a commuting differential operator that shares the same eigenfunctions. In this report, we develop an efficient numerical algorithm for evaluating the eigendecomposition of the integral operator to full relative precision, using the eigendecomposition of the differential operator. With our algorithm, the Tracy-Widom distribution can be evaluated to full absolute precision everywhere rapidly, and, furthermore, its right tail can be computed to full relative precision.

On the Evaluation of the Eigendecomposition of the Airy Integral Operator

Zewen Shen[†] and Kirill Serkh[‡◇]

University of Toronto NA Technical Report
April 26, 2021

◇ This author's work was supported in part by the NSERC Discovery Grants RGPIN-2020-06022 and DGECR-2020-00356.

† Dept. of Computer Science, University of Toronto, Toronto, ON M5S 2E4
‡ Dept. of Math. and Computer Science, University of Toronto, Toronto, ON M5S 2E4

Contents

1 Introduction

Recently, random matrix theory has become one of the most exciting fields in probability theory, and has been applied to problems in physics [12], high-dimensional statistics [18], wireless communications [7], finance [4], etc. The Tracy-Widom distribution, describing the normalized largest eigenvalue of a random Hermitian matrix, is one of the most important probability distributions in random matrix theory. There are generally two ways of calculating the Tracy-Widom distribution to high accuracy numerically: one, using the Painlevé representation of the distribution to reduce the calculation to solving a nonlinear ordinary differential equation (ODE) numerically, and the other, using the determinantal representation of the distribution to reduce the calculation to an eigenproblem for an integral operator. In the celebrated work [22], the Tracy-Widom distribution was shown to be representable as an integral of a solution to a certain nonlinear ODE called the Painlevé II equation. This nonlinear ODE can be solved to relative accuracy numerically, but solving it to high accuracy is extremely expensive, since it generally requires multi-precision arithmetic [19]. On the other hand, the method based on the determinantal representation uses the fact that the Tracy-Widom distribution can be written in the following Fredholm determinantal form:

$$F_2(s) = \det(I - K_{\mathrm{Ai}}|_{L^2[s,\infty)}), \tag{1}$$

where $K_{\mathrm{Ai}}|_{L^2[s,\infty)}$ denotes the integral operator on $L^2[s,\infty)$ with kernel

$$K_{Ai}(x,y) = \int_s^\infty \mathrm{Ai}(x+z-s)\mathrm{Ai}(z+y-s)\,\mathrm{d}z, \tag{2}$$

where $\mathrm{Ai}(x)$ is the Airy function of the first kind (see [22, 11] for the derivations). It's known that the cumulative distribution function (CDF) and the probability density function (PDF) of the distribution can be computed from the spectrum of the integral operator $\mathcal{G}_s|_{L^2[s,\infty)}$, where $\mathcal{G}_s[f](x) = \int_s^\infty \mathrm{Ai}(x+y-s)f(y)\,\mathrm{d}y$, since $K_{\mathrm{Ai}}|_{L^2[s,\infty)} = \mathcal{G}_s^2$. If the eigenvalues of the integral operator $\mathcal{G}_s$ are computed directly, they can be known only to absolute precision since $\mathcal{G}_s$ is a compact integral operator. Furthermore, the number of degrees of freedom required to discretize $\mathcal{G}_s$ increases when the kernel is oscillatory (as $s \to -\infty$).

In this report, we present a new method for computing the eigendecomposition of the integral operator $\mathcal{G}_s$. It exploits the remarkable fact that the integral operator $\mathcal{G}_s$ admits a commuting differential operator, which shares the same eigenfunctions. In our method, we compute the spectrum and the eigenfunctions of the differential operator by computing the eigenvalues and eigenvectors of a banded eigenproblem. Since the eigenproblem is banded, the eigendecomposition can be done very quickly (an eigensolver for an $n \times n$ banded matrix only requires $\mathcal{O}(n^2)$ operations, while for a dense matrix it requires $\mathcal{O}(n^3)$ operations). Furthermore, since the eigenproblem is banded, we compute the eigenvalues and eigenvectors to full relative precision. We use the eigenvectors to compute the spectrum of the integral operator $\mathcal{G}_s$, also to full relative precision. As a result, our method computes the Tracy-Widom distribution to full absolute precision rapidly for all s, including in the left tail. Moreover, it evaluates both the CDF and PDF to relative precision for $s > -5$, including in the right tail.

Integral operators like $\mathcal{G}_s$, which admit commuting differential operators, are known as *bispectral operators* (see [5]). One famous example of a bispectral operator is the truncated Fourier transform, which was investigated by Slepian and his collaborators in the 60's [21]; its eigenfunctions are known as prolate spheroidal wavefunctions. We note that, unlike prolates, the eigenfunctions of the operator $\mathcal{G}_s$ are relatively unexamined: "In the case of the Airy kernel ... the differential equation did not receive much attention and its solutions are not known" [15]. In this report, we also characterize these previously unstudied eigenfunctions.

1.1 Previous work on the numerical evaluation of the Tracy-Widom distribution

In this section, we describe several previously proposed methods for computing the Tracy-Widom distribution. In general, there are two popular methods: one is based on solving for a Painlevé transcendent [9, 10], and the other is based on approximating a Fredholm determinant of an integral operator [3]. For a long time, the former way was regarded as the rule of thumb for the numerical computation of the distribution. The Fredholm determinant method was introduced as an alternative by Bornemann in [3]. Bornemann points out that the numerical evaluation of the Painlevé transcendent via solving an initial value problem (IVP) is "more involved than one would think at first sight" [2], since the IVP is highly sensitive to the initial condition. Although one may remedy the numerical instability by formulating a boundary value problem (BVP) based on the IVP and the asymptotic expansion of the corresponding connection formulas, it requires deep analytic knowledge and parameter tuning [8, 2]. On the other hand, one can approximate the Fredholm determinant via some quadrature rule in ten lines of code [3], although the time complexity is not ideal, especially when one is interested in the left tail of the distribution. When the distribution is not needed to full accuracy, other effective methods can be used, including methods based on a shifted Gamma distribution approximation [6], and direct statistical simulations [10]. Finally, we note that all the existing methods, except [19], which tabulates the PDF and the CDF to relative accuracy by solving an ODE numerically using a Taylor series method in multi-precision arithmetic, can at most achieve absolute precision in evaluating the Tracy-Widom distribution.

2 Mathematical Preliminaries

2.1 Airy function of the first kind

The Airy function of the first kind is the solution to the differential equation

$$\frac{d^2y}{dx^2} - xy = 0, \tag{3}$$

for all $x \in \mathbb{R}$, that decays for large x. It can also be written in an integral representation

$$\mathrm{Ai}(x) = \frac{1}{\pi}\int_0^\infty \cos\Big(\frac{t^3}{3} + xt\Big)\,\mathrm{d}t. \tag{4}$$

Remark 2.1. One can extend the definition of $\mathrm{Ai}(x)$ to the complex plane and show that it is an entire function. Consequentially, it is an analytic function on the real axis.

Remark 2.2. As $x \to +\infty$,

$$\mathrm{Ai}(x) \sim \frac{e^{-\frac{2}{3}x^{3/2}}}{2\pi^{1/2}x^{1/4}}. \tag{5}$$

2.2 Laguerre polynomials

The Laguerre polynomials, denoted by $L_n\colon [0,\infty) \to \mathbb{R}$, are defined by the following three-term recurrence relation for any $k \geq 1$ (see [1]):

$$L_{k+1}(x) = \frac{(2k+1-x)L_k(x) - kL_{k-1}(x)}{k+1}, \tag{6}$$

with the initial conditions

$$L_0(x) = 1, \quad L_1(x) = 1 - x. \tag{7}$$

The polynomials defined by the formulas (6) and (7) are an orthonormal basis in the Hilbert space induced by the inner product $\langle f, g\rangle = \int_0^\infty e^{-x} f(x)g(x)\,\mathrm{d}x$, i.e.,

$$\langle L_n, L_m\rangle = \int_0^\infty e^{-x} L_n(x)L_m(x)\,\mathrm{d}x = \delta_{n,m}. \tag{8}$$

In addition, Laguerre polynomials are solutions of Laguerre's equation:

$$xy'' + (1-x)y' + ny = 0. \tag{9}$$

We find it useful to use the scaled Laguerre functions defined below.

Definition 2.1. Given a positive real number a, the scaled Laguerre functions, denoted by $h_n^a\colon [0,\infty) \to \mathbb{R}$, are defined by

$$h_n^a(x) = \sqrt{a}e^{-\frac{ax}{2}} L_n(ax). \tag{10}$$

Remark 2.3. The scaled Laguerre functions $h_n^a(x)$ are an orthonormal basis in $L^2[0,\infty)$, i.e.,

$$\int_0^\infty h_n^a(x)h_m^a(x)\,\mathrm{d}x = \delta_{n,m}. \tag{11}$$

The following two theorems directly follow from the results for Laguerre polynomials in, for example, [1].

Theorem 2.1. *Given a positive real number a and a non-negative integer n,*

$$xh_n^a(x) = \frac{1}{a}\big(-nh_{n-1}^a(x) + (2n+1)h_n^a(x) - (n+1)h_{n+1}^a(x)\big), \tag{12}$$

$$\begin{aligned} x^2h_n^a(x) = \frac{1}{a^2}\big(&n(n-1)h_{n-2}^a(x) - 4n^2h_{n-1}^a(x) + (6n^2+6n+2)h_n^a(x) \\ &- 4(1+n)^2h_{n+1}^a(x) + (n+1)(n+2)h_{n+2}^a(x)\big). \end{aligned} \tag{13}$$

Theorem 2.2. *Given a positive real number a and a non-negative integer n,*

$$\frac{d}{dx}h_n^a = -\frac{a}{2}h_n^a - a\sum_{k=0}^{n-1} h_k^a, \tag{14}$$

$$\frac{d^2}{dx^2}h_n^a = \frac{a^2}{4}h_n^a + a^2\sum_{k=0}^{n-1}(n-k)h_k^a. \tag{15}$$

The following corollary is a direct result of (14).

Corollary 2.3. *Given a positive real number a and a non-negative integer n,*

$$\frac{d}{dx}h_n^a - \frac{d}{dx}h_{n-1}^a = -\frac{a}{2}h_n^a - \frac{a}{2}h_{n-1}^a. \tag{16}$$

Observation 2.4. The scaled Laguerre functions $h_n^a(x)$ are solutions of the following ODE on the interval $[0,\infty)$:

$$\frac{d}{dx}\Big(x\frac{d}{dx}h_n^a\Big) - \frac{a}{4}(ax - 4n - 2)h_n^a = 0. \tag{17}$$

Definition 2.2. For any positive real number a, let $\mathcal{M}_c : L^2[0,\infty) \to L^2[0,\infty)$ denote the differential operator defined by

$$\mathcal{M}_a[f] = -\frac{d}{dx}\Big(x\frac{d}{dx}f\Big) + \frac{1}{4}a^2xf. \tag{18}$$

By (17), we observe that, h_n^a solves the Sturm-Liouville eigenproblem of $\mathcal{M}_a$ with singular points $x = 0$ and $x = \infty$, and its corresponding eigenvalue is $a(n + \frac{1}{2})$.

The following theorem, proven (in a slightly different form) in [24], describes the decaying property of the expansion coefficients in the Laguerre polynomial basis.

Theorem 2.4. *Suppose $f \in C^k([0,\infty))$ where $k \geq 1$, and f satisfies*

$$\lim_{x\to\infty} e^{-x/2}x^{j+1}f^{(j)}(x) = 0, \tag{19}$$

$$V = \sqrt{\int_0^\infty x^{k+1}e^{-x}(f^{(k+1)}(x))^2\,\mathrm{d}x} < \infty, \tag{20}$$

for $j = 0, 1, \ldots, k$. Suppose further that $a_n = \int_0^\infty e^{-x}f(x)L_n(x)\,\mathrm{d}x$. Then,

$$|a_n| \leq \frac{V}{\sqrt{n(n-1)\ldots(n-k)}} = \mathcal{O}(\frac{1}{n^{(k+1)/2}}),\ \textit{for } n > k, \tag{21}$$

and

$$\|f(x) - \sum_{n=0}^{N} a_nL_n(x)\| \to 0,\ \textit{as } N \to \infty, \tag{22}$$

where $\|\cdot\|$ represents the $L^2([0,\infty))$ norm with the weight function e^{-x}.

The following corollary extends the theorem above to the case where the Laguerre polynomials are replaced by scaled Laguerre functions.

Corollary 2.5. *Suppose that $a \in \mathbb{R}$ and $a > 0$. Suppose further that $g \in C^k([0,\infty))$ for some $k \geq 1$, and define $f(x) = \frac{1}{\sqrt{a}}e^{x/2}g(x/a)$. Assume finally that f satisfies*

$$\lim_{x\to\infty} e^{-x/2}x^{j+1}f^{(j)}(x) = 0, \tag{23}$$

$$V = \sqrt{\int_0^\infty x^{k+1}e^{-x}(f^{(k+1)}(x))^2\,\mathrm{d}x} < \infty, \tag{24}$$

for $j = 0, 1, \ldots, k$, and let $b_n = \int_0^\infty g(x) h_n^a(x)\,\mathrm{d}x$. Then,

$$|b_n| \le \frac{V}{\sqrt{n(n-1)\ldots(n-k)}} = \mathcal{O}(\frac{1}{n^{(k+1)/2}}),\ \textit{for } n > k, \tag{25}$$

and

$$\|g(x) - \sum_{n=0}^{N} b_n h_n^a(x)\| \to 0,\ \textit{as } N \to \infty, \tag{26}$$

where $\|\cdot\|$ represents the $L^2([0,\infty))$ norm with the weight function 1.

Proof. By definition,

$$\begin{aligned} |b_n| &= \Big| \int_0^\infty h_n^a(x) g(x)\,\mathrm{d}x \Big| = \Big| \int_0^\infty \sqrt{a} e^{-\frac{ax}{2}} L_n(ax) g(x)\,\mathrm{d}x \Big| \\ &= \Big| \int_0^\infty \frac{1}{\sqrt{a}} e^{-x/2} L_n(x) g(x/a)\,\mathrm{d}x \Big| = \Big| \int_0^\infty e^{-x} L_n(x) f(x)\,\mathrm{d}x \Big| \\ &= |a_n| \le \frac{V}{\sqrt{n(n-1)\ldots(n-k)}}, \end{aligned} \tag{27}$$

where a_n is defined in the same way as Theorem 2.4. Thus, (25) is proved.

To prove (26), note that

$$\begin{aligned} \|g(x) - \sum_{n=0}^{N} b_n h_n^a(x)\|^2 &= \int_0^\infty (g(x) - \sum_{n=0}^{N} b_n \sqrt{a} e^{-ax/2} L_n(ax))^2\,\mathrm{d}x \\ &= \int_0^\infty (g(\frac{y}{a}) - \sum_{n=0}^{N} b_n \sqrt{a} e^{-y/2} L_n(y))^2 \frac{1}{a}\,\mathrm{d}y \\ &= \int_0^\infty (\frac{1}{\sqrt{a}} g(\frac{y}{a}) - \sum_{n=0}^{N} b_n e^{-y/2} L_n(y))^2\,\mathrm{d}y \\ &= \int_0^\infty e^{-y} (f(y) - \sum_{n=0}^{N} b_n L_n(y))^2\,\mathrm{d}y \\ &\le \int_0^\infty (f(y) - \sum_{n=0}^{N} b_n L_n(y))^2\,\mathrm{d}y \\ &= \|f(x) - \sum_{j=0}^{n} a_n L_n(x)\|^2 \to 0, \end{aligned} \tag{28}$$

where the last equality holds by combining Theorem 2.4 and the fact that $b_n = a_n$ (see formula (27)). ■

2.3 Airy integral operator and its associated integral operator

In this subsection, we define the Airy integral operator, including its eigenvalues and eigenfunctions. Its associated integral operator is introduced as well.

Definition 2.3. Given a real number c, let $\mathcal{G}_c\colon L^2[c,\infty) \to L^2[c,\infty)$ denote the Airy integral operator defined by

$$\mathcal{G}_c[f](x) = \int_c^\infty \mathrm{Ai}(x+y-c)f(y)\,\mathrm{d}y, \quad x \geq c. \tag{29}$$

Let $\mathcal{T}_c\colon L^2[0,\infty) \to L^2[0,\infty)$ denote the integral operator defined by

$$\mathcal{T}_c[f](x) = \int_0^\infty \mathrm{Ai}(x+y+c)f(y)\,\mathrm{d}y, \quad x \geq 0. \tag{30}$$

We will refer $\mathcal{T}_c$ as the associated Airy integral operator.

Obviously, both $\mathcal{G}_c$ and $\mathcal{T}_c$ are compact. It is easy to see that $\mathcal{G}_c^2 = K_{\mathrm{Ai}}|_{L^2[c,\infty)}$ (see formula (2)).

We will denote the eigenvalues of $\mathcal{G}_c$ by $\mu_{0,c}, \mu_{1,c}, \ldots, \mu_{n,c}, \ldots$ ordered so that $|\mu_{j-1,c}| \geq |\mu_{j,c}|$ for all $j \in \mathbb{N}^+$; denote the eigenvalues of $\mathcal{T}_c$ by $\lambda_{0,c}, \lambda_{1,c}, \ldots, \lambda_{n,c}, \ldots$ ordered so that $|\lambda_{j-1,c}| \geq |\lambda_{j,c}|$ for all $j \in \mathbb{N}^+$. For each non-negative integer j, let $\phi_{j,c}$ and $\psi_{j,c}$ denote the j-th eigenfunctions of $\mathcal{G}_c$ and $\mathcal{T}_c$, respectively, so that

$$\mu_{j,c}\phi_{j,c}(x) = \int_c^\infty \mathrm{Ai}(x+y-c)\phi_{j,c}(y)\,\mathrm{d}y, \quad x \in [c,\infty), \tag{31}$$

$$\lambda_{j,c}\psi_{j,c}(x) = \int_0^\infty \mathrm{Ai}(x+y+c)\psi_{j,c}(y)\,\mathrm{d}y, \quad x \in [0,\infty). \tag{32}$$

In this report, we normalize the eigenfunctions, such that $\|\phi_{j,c}\|_2 = \|\psi_{j,c}\|_2 = 1$ for any real positive number c and non-negative integer j.

Note that $\mathcal{T}_c$ and $\mathcal{G}_c$ share the same eigenvalues and eigenfunctions up to a translation, i.e.,

$$\lambda_{j,c} = \mu_{j,c}, \tag{33}$$

$$\psi_{j,c}(x) = \phi_{j,c}(x+c), \quad x \geq 0. \tag{34}$$

It follows that if we are interested in $\mathcal{G}_c$, it's equivalent to investigate $\mathcal{T}_c$. Note that the operator $\mathcal{T}_c$ is more convenient to study than the operator $\mathcal{G}_c$, as its domain is invariant under the change of c. Therefore, we will only study $\mathcal{T}_c$ in this report.

Remark 2.5. For simplicity, we will use λ_j and ψ_j to denote the eigenvalue and the eigenfunction when there is no ambiguity.

2.4 Commuting differential operator of the associated Airy integral operator

Definition 2.4. Given a real number c, let $\mathcal{L}_c\colon L^2[0,\infty) \to L^2[0,\infty)$ denote the Sturm-Liouville operator defined by

$$\mathcal{L}_c[f](x) = -\frac{d}{dx}\Big(x\frac{d}{dx}f\Big) + x(x+c)f. \tag{35}$$

Obviously, $\mathcal{L}_c$ is self-adjoint (more specifically, it's a singular Sturm-Louville operator with singular points $x = 0$ and $x = \infty$). It is fairly straightforward to show that $\mathcal{L}_c$ commutes with $\mathcal{T}_c$ and their eigenvalues have multiplicity one. Thus, $\mathcal{L}_c$ and $\mathcal{T}_c$ share the same set of eigenfunctions. The following theorem formalizes this statement (see [22, 13]).

Theorem 2.6. *For any real number c, there exists a strictly increasing sequence of positive real numbers $\chi_{0,c}, \chi_{0,c}, \dots$ such that, for each $m \geq 0$, the differential equation*

$$\frac{d}{dx}\Big(x\frac{d}{dx}\psi_{m,c}\Big) - (x^2 + cx - \chi_{m,c})\psi_{m,c} = 0 \tag{36}$$

has a solution $\psi_{m,c}$ that is continuous on the interval $[0,\infty)$. For each $m \geq 0$, the function $\psi_{m,c}$ is exactly the m-th eigenfunction of the integral operator $\mathcal{T}_c$.

Remark 2.6. The equation (36) can also be written as

$$\mathcal{L}_c[\psi_{m,c}] = \chi_{m,c}\psi_{m,c}. \tag{37}$$

Remark 2.7. The numerical evaluation of high-order eigenfunctions via the discretization of the integral operator $\mathcal{T}_c$ is highly inaccurate due to its exponentially decaying eigenvalues. On the contrary, the Sturm-Liouville operator $\mathcal{L}_c$ has a growing and well-separated spectrum and is numerically much more tractable. Therefore, $\mathcal{L}_c$ is an important tool for computing eigenvalues and eigenvectors of $\mathcal{T}_c$.

2.5 Numerical tools for five-diagonal matrices

2.5.1 Eigensolver

Given a symmetric five-diagonal matrix, it can be reduced to a tridiagonal matrix using the algorithm in [20]. Once it is in tridiagonal form, a standard Q-R (or Q-L) algorithm can then be used to solve for all its eigenvalues to absolute precision.

Remark 2.8. The time complexity of the reduction and Q-R algorithm are both $\mathcal{O}(n^2)$ for a symmetric five-diagonal matrix of size $n \times n$.

2.5.2 Shifted inverse power method

Suppose that $N \geq 0$ is an integer, and that A is an $N \times N$ real symmetric matrix. Suppose also that $\sigma_1 < \sigma_2 < \cdots < \sigma_N$ are the eigenvalues of A. The inverse power method iteratively finds the eigenvalue σ_k and $v_k \in \mathbb{R}^N$, provided an approximation λ to σ_k is given, and that

$$|\lambda - \sigma_k| < \max\{|\lambda - \sigma_j|\colon j \neq k\}. \tag{38}$$

Each inverse power iteration solves the linear system

$$(A - \lambda_j I)x = w_j, \tag{39}$$

where λ_j and $w_j \in \mathbb{R}^n$ are the approximations to σ_k and v_k, respectively, after j iterations; the number λ_j is usually referred to as a "shift". The approximations λ_{j+1} and $w_{j+1} \in \mathbb{R}^N$ are evaluated from x via the formulas

$$w_{j+1} = \frac{x}{\|x\|}, \quad \lambda_{j+1} = w_{j+1}^T A w_{j+1} \tag{40}$$

(see, for example, [17, 23] for more details).

Remark 2.9. For symmetric matrices, the shifted inverse power method converges cubically in the vicinity of the solution, and each iteration requires $\mathcal{O}(n)$ operations for a tridiagonal or a five-diagonal matrix (see [14, 17, 23]).

3 Analytical apparatus

In this section, we introduce several analytical results which we will use to develop the numerical algorithm of this report. We denote the eigenfunctions of the eigenfunctions of the operators $\mathcal{T}_c$ and $\mathcal{L}_c$ by $\psi_{n,c}$ (see Sections 2.3, 2.4), and represent them in the basis of scaled Laguerre functions h_k^a (see Section 2.2). Finally, we denote the eigenvalues of the integral operators $\mathcal{T}_c$, $\mathcal{G}_c$ by $\lambda_{n,c}$.

3.1 The commuting differential operator in the basis of scaled Laguerre functions

Theorem 3.1. *For any positive real number a, real number c, and non-negative integer k,*

$$\begin{aligned}
\mathcal{L}_c[h_k^a](x) = \frac{1}{4a^2}\Big(&4k(k-1)h_{k-2}^a(x) \\
&+ k(a^3 - 4ac - 16k)h_{k-1}^a(x) \\
&+ (8 + a^3 + 4ac + 24k + 2a^3k + 8ack + 24k^2)h_k^a(x) \\
&+ (k+1)\big(a^3 - 4ac - 16(k+1)\big)h_{k+1}^a(x) \\
&+ 4(k+1)(k+2)h_{k+2}^a(x)\Big),
\end{aligned} \tag{41}$$

where $x \in [0, \infty)$.

Proof. By definition,

$$\mathcal{L}_c[h_k^a](x) = -\frac{d}{dx}\Big(x\frac{d}{dx}h_k^a(x)\Big) + x(x+c)h_k^a(x). \tag{42}$$

By applying (17), terms involving derivatives of $h_n^a(x)$ on the right side of (42) disappear. Finally, we reduce the remaining $xh_k^a(x), x^2h_k^a(x)$ terms to $h_k^a(x)$ via (12), (13). ■

Remark 3.1. Although $h_{k-2}^a(x), h_{k-1}^a(x)$ may be undefined when $k = 0, 1$, the theorem still holds since in that case, the coefficients of $h_{k-2}^a(x), h_{k-1}^a(x)$ in (41) will be zero.

3.2 Decay of the expansion coefficients of the eigenfunctions

Theorem 3.2. *Suppose that $a, c \in \mathbb{R}$ and $a > 0$. Suppose further that $\beta_k^{(m)} = \int_0^\infty \psi_{m,c}(x) h_k^a(x)\,\mathrm{d}x$ for $k = 0, 1, \ldots$. Then, $|\beta_k^{(m)}|$ decays super-algebraically as k goes to infinity.*

Proof.

$$\begin{aligned}
|\beta_k^{(m)}| &= \frac{1}{|\lambda_m|}\left| \int_0^\infty \psi_{m,c}(y)\Big(\int_0^\infty \mathrm{Ai}(y+x+c) h_k^a(x)\,\mathrm{d}x\Big)\,\mathrm{d}y\right| \\
&\le \frac{1}{|\lambda_m|}\|\psi_{m,c}(y)\|_{L^2(0,\infty)} \left\| \int_0^\infty \mathrm{Ai}(y+x+c) h_k^a(x)\,\mathrm{d}x\right\|_{L^2(0,\infty)} \\
&= \frac{1}{|\lambda_m|}\left\| \int_0^\infty \mathrm{Ai}(y+x+c) h_k^a(x)\,\mathrm{d}x\right\|_{L^2(0,\infty)}, \qquad (43)
\end{aligned}$$

by Cauchy-Schwartz inequality and the fact that $\|\psi_{m,c}(y)\|_{L^2(0,\infty)} = 1$.

Define $g(x) = \mathrm{Ai}(y + x + c)$ for some constants $y \ge 0, c \in \mathbb{R}$. By Remark 2.2, for any real number $a > 0$, it's clear that $f(x) = \frac{1}{\sqrt{a}} e^{x/2} g(x/a)$ satisfies the conditions (23), (24) in Corollary 2.5. As g is analytic, we have that $g \in C^p([0,\infty))$ for any non-negative integer p. Therefore, by Corollary 2.5, $|\beta_k^{(m)}|$ decays super-algebraically as k goes to infinity. ■

3.3 Recurrence relation involving the associated Airy integral operator acting on scaled Laguerre functions of different orders

Theorem 3.3. *Given a real number $a > 0$, a real number s, and a non-negative integer n, define*

$$H_n^a := \int_0^\infty Ai(y+s) h_n^a(y)\,\mathrm{d}y = \sqrt{a}\int_0^\infty Ai(y+s) e^{-\frac{ay}{2}} L_n(ay)\,\mathrm{d}y. \qquad (44)$$

Then

$$\begin{aligned}
&(n-1)H_{n-2}^a - (4n - 1 + as - \frac{1}{4}a^3)H_{n-1}^a + (6n + 3 + 2as + \frac{1}{2}a^3)H_n^a \\
&\qquad - (4n + 5 + as - \frac{1}{4}a^3)H_{n+1}^a + (n+2)H_{n+2}^a = 0, \qquad (45)
\end{aligned}$$

for $n = 1, 2, \ldots$.

Proof. By combining the recurrence relation of Laguerre polynomials (see (6)) and the definition of the Airy function (see (3)), we have

$$\begin{aligned}
H_{n+1}^a &= \int_0^\infty \mathrm{Ai}(y+s) h_{n+1}^a(y)\,\mathrm{d}y \qquad (46)\\
&= \int_0^\infty \mathrm{Ai}(y+s)\frac{(2n+1-ay)h_n^a(y) - n h_{n-1}^a(y)}{n+1}\,\mathrm{d}y \qquad (47)\\
&= \frac{2n+1}{n+1}H_n^a - \frac{n}{n+1}H_{n-1}^a - \frac{a}{n+1}\int_0^\infty y\mathrm{Ai}(y+s) h_n^a(y) dy \qquad (48)\\
&= \frac{2n+1+as}{n+1}H_n^a - \frac{n}{n+1}H_{n-1}^a - \frac{a}{n+1}\int_0^\infty \mathrm{Ai}''(y+s) h_n^a(y)\,\mathrm{d}y, \qquad (49)
\end{aligned}$$

for any non-negative integer n. By applying integration by parts twice to the last term in (49), we get

$$\int_0^\infty \mathrm{Ai}''(y+s)h_n^a(y)\,\mathrm{d}y = -\sqrt{a}\mathrm{Ai}'(s) - a\sqrt{a}(\frac{1}{2}+n)\mathrm{Ai}(s) + \int_0^\infty \mathrm{Ai}(y+s)(h_n^a(y))''\,\mathrm{d}y. \tag{50}$$

By (15), the last term in (50) becomes

$$\int_0^\infty \mathrm{Ai}(y+s)(h_n^a(y))''\,\mathrm{d}y = a^2\int_0^\infty \mathrm{Ai}(y+s)\Big(\frac{1}{4}h_n^a(y) + \sum_{k=0}^{n-1}(n-k)h_k^a(y)\Big)\,\mathrm{d}y \tag{51}$$

$$= a^2\big(\frac{1}{4}H_n^a + \sum_{k=0}^{n-1}(n-k)H_k^a\big). \tag{52}$$

Thus, by multiplying both sides of (49) by $n+1$, and combining (50), (52), we have

$$nH_{n-1}^a - (2n+1+as-\frac{1}{4}a^3)H_n^a + (n+1)H_{n+1}^a + a^3\sum_{k=0}^{n-1}(n-k)H_k^a = a\sqrt{a}\Big(\mathrm{Ai}'(s) + a(\frac{1}{2}+n)\mathrm{Ai}(s)\Big), \tag{53}$$

for $n = 0, 1, 2, \ldots$.

We can write (53) equivalently as

$$(n-1)H_{n-2}^a - (2n-1+as-\frac{1}{4}a^3)H_{n-1}^a + nH_n^a + a^3\sum_{k=0}^{n-2}(n-1-k)H_k^a = a\sqrt{a}\Big(\mathrm{Ai}'(s) + a(-\frac{1}{2}+n)\mathrm{Ai}(s)\Big), \tag{54}$$

for $n = 1, 2, 3, \ldots$, or

$$(n+1)H_n^a - (2n+3+as-\frac{1}{4}a^3)H_{n+1}^a + (n+2)H_{n+2}^a + a^3\sum_{k=0}^{n}(n+1-k)H_k^a = a\sqrt{a}\Big(\mathrm{Ai}'(s) + a(\frac{3}{2}+n)\mathrm{Ai}(s)\Big), \tag{55}$$

for $n = -1, 0, 1, \ldots$.

Finally, noticing that

$$\sum_{k=0}^{n-2}(n-1-k)H_k^a - 2\sum_{k=0}^{n-1}(n-k)H_k^a + \sum_{k=0}^{n}(n+1-k)H_k^a = H_n^a, \tag{56}$$

equation (54), minus two times equation (53), plus equation (55), gives the identity that we need. ■

3.4 Recurrence relation between the eigenvalues of the integral operator

The following theorem follows from formula (117) in the proof of Theorem 6.4.

Theorem 3.4. *For any non-negative integers m, n,*

$$\frac{\lambda_m}{\lambda_n} = \frac{\int_0^\infty \psi_n'(x)\psi_m(x)\,\mathrm{d}x}{\int_0^\infty \psi_n(x)\psi_m'(x)\,\mathrm{d}x}. \tag{57}$$

4 Numerical algorithms

4.1 Discretization of the eigenfunctions

The algorithm for the evaluation of the eigenfunctions $\psi_{j,c}$ is based on the expression of those functions as a series of scaled Laguerre functions (see (10)) of the form

$$\psi_{j,c}(x) = \sum_{k=0}^{\infty} \beta_k^{(j)} h_k^a(x), \tag{58}$$

where the coefficients $\beta_k^{(j)}$ depends on the parameter c.

Remark 4.1. By orthogonality of the scaled Laguerre functions and the fact that $\|\psi_{j,c}\|_2^2 = 1$, we conclude that

$$\sum_{k=0}^{\infty} \big(\beta_k^{(j)}\big)^2 = 1. \tag{59}$$

Now we substitute the expansion (58) into (37), which gives us

$$\sum_{k=0}^{\infty} \beta_k^{(j)} \mathcal{L}_c[h_k^a] = \chi_{n,c} \sum_{k=0}^{\infty} \beta_k^{(j)} h_k^a. \tag{60}$$

It follows from (41) that the left side of (60) can be expanded into a summation that only involves $h_0^a, h_1^a, \dots$. By linear independence of the scaled Laguerre functions and (41), the sequence $\beta_0^{(j)}, \beta_1^{(j)}, \dots$ satisfies the recurrence relation

$$\begin{aligned}
A_{0,0}\cdot\beta_0^{(j)} + A_{0,1}\cdot\beta_1^{(j)} + A_{0,2}\cdot\beta_2^{(j)} &= \chi_{j,c}\cdot\beta_0^{(j)},\\
A_{1,0}\cdot\beta_0^{(j)} + A_{1,1}\cdot\beta_1^{(j)} + A_{1,2}\cdot\beta_2^{(j)} + A_{1,3}\cdot\beta_3^{(j)} &= \chi_{j,c}\cdot\beta_1^{(j)},\\
A_{k,k-2}\cdot\beta_{k-2}^{(j)} + A_{k,k-1}\cdot\beta_{k-1}^{(j)} + A_{k,k}\cdot\beta_k^{(j)}&\\
+A_{k,k+1}\cdot\beta_{k+1}^{(j)} + A_{k,k+2}\cdot\beta_{k+2}^{(j)} &= \chi_{j,c}\cdot\beta_k^{(j)},
\end{aligned} \tag{61}$$

for $k = 2, 3, \dots$, where $A_{k,k}, A_{k,k+1}, A_{k,k+2}$ are defined via the formulas

$$\begin{aligned}
A_{k,k} &= \frac{1}{4a^2}(8 + a^3 + 4ac + 24k + 2a^3k + 8ack + 24k^2),\\
A_{k,k+1} &= A_{k+1,k} = \frac{1}{4a^2}(k+1)\big(a^3 - 4ac - 16(k+1)\big),\\
A_{k,k+2} &= A_{k+2,k} = \frac{1}{a^2}(k+1)(k+2),
\end{aligned} \tag{62}$$

for $k = 0, 1, \dots$. Note that (61) can be written in the form of the following linear system:

$$(A - \chi_{j,c} I) \cdot \left(\beta_0^{(j)}, \beta_1^{(j)}, \dots\right)^T = 0, \tag{63}$$

where I is the infinite identity matrix, and the non-zero entries of the infinite symmetric matrix A are given above.

Suppose that k is a non-negative integer. Although the matrix A is infinite, and its entries do not decay with increasing row or column number, the components of each eigenvector $\beta^{(k)}$ decay super-algebraically (see Theorem 3.2). More specifically, the absolute value of components of the k-th eigenvector will look like a bell-shaped curve centered at the k-th entry of the eigenvector. Therefore, if we need to evaluate the first $n+1$ eigenvalues $\chi_{0,c}, \chi_{1,c}, \dots, \chi_{n,c}$ and eigenvectors $\beta^{(0)}, \beta^{(1)}, \dots, \beta^{(n)}$ numerically, we can replace the infinite matrix A with its $(N+1) \times (N+1)$ upper left square submatrix, where $N = \mathcal{O}(n)$ is sufficiently large, which results in a symmetric five-diagonal eigenproblem. It follows that we can replace the series expansion (58) with a truncated one:

$$\psi_{j,c}(x) = \sum_{k=0}^{N} \beta_k^{(j)} h_k^a(x), \tag{64}$$

for $j = 0, 1, \dots, n$.

Assuming that we are interested in the first $n+1$ eigenfunctions of the differential operator $\mathcal{L}_c$, it's important to pick the scaling factor a such that $\psi_{n,c}$ gets best approximated, in the sense that the bell-shape of the expansion coefficients of $\psi_{n,c}$ are concentrated around $k = n$. By (59), it follows that a considerably smaller matrix will be required to calculate the $\psi_{n,c}$ accurately, compared with other choices of a. Note that this choice of a is not optimal for the rest of the n eigenfunctions, especially for the leading ones $\psi_{0,c}, \psi_{1,c}, \dots$. However, in practice, if we can represent $\psi_{n,c}$ accurately, then the rest of the n eigenfunctions can be represented with at most the same number of the basis functions. Therefore, we only need to choose a to efficiently represent $\psi_{n,c}$.

To get a best approximation for $\psi_{n,c}$, we want the behaviour of h_n^a to be similar to $\psi_{n,c}$. Notice that by (17), (36), the two ODEs satisfied by h_n^a, $\psi_{n,c}$ only differ by the coefficient of the zero-th order term. It follows that the turning point of h_n^a is

$$x = \frac{2(n-1)}{a}, \tag{65}$$

while the turning point of $\psi_{n,c}$ is

$$x = \frac{-c + \sqrt{c^2 + 4\chi_{n,c}}}{2}. \tag{66}$$

Matching the turning points of the two solutions, we get the following approximation to the optimal a:

$$a = \frac{4(2n-1)}{-c + \sqrt{c^2 + 4\chi_{n,c}}}. \tag{67}$$

With this choice of a, β_k decays quickly for $k \geq n$, for the entire range of $c \in \mathbb{R}$. We note that, the decay behaviour of β_k is highly sensitive to the choice of a; other values of a will often cause β_k to oscillate for a long time before it decays. To simplify the notation, we will use $h_k(x)$ to denote $h_k^a(x)$ with the optimal choice for a in the rest of the report.

Observation 4.2. By applying the method of least squares to our numerical experiments, $\chi_{n,c} \approx 19.3c + 11.1n + 1.19 \cdot 10^{-2}n^2 + 7.4 \cdot 10^{-5}cn^2$ turns out to be a good approximation to the eigenvalues of the differential operator for $c \in [-50, 50], n = 0, 1, \ldots, 800$.

Observation 4.3. Empirically, $\beta_k \approx 0$ for $k \geq N$, where $N = 1.1n + |c| + 100$.

Observation 4.4. One might hope that, by a certain selection of basis functions, it's possible to split this five-diagonal eigenproblem into two tridiagonal eigenproblems (see, for example, [17, 14]). However, it turns out that none of the classical orthogonal polynomials (Laguerre polynomials, Hermite polynomials, or their rescaled versions) defined on the interval $[0, \infty)$ have the capability to split our five-diagonal eigenproblem.

Observation 4.5. When c is negative, the leading few eigenvalues, say, $\chi_{0,c}, \chi_{1,c}, \ldots, \chi_{n',c}$, are negative, where n' is usually smaller than 100 in practical situations. In this case, provided one is only interested in the first n eigenfunctions, where $n - 1 \leq n'$, it would appear that the calculation of $\sqrt{c^2 + 4\chi_{n,c}}$ in formula (67) may fail, since $c^2 + 4\chi_{n,c}$ can be negative. However, $c^2 + 4\chi_{n,c}$ turns out to always be positive. To estimate a, we use an approximation to $\chi_{n,c}$, for which the quantity $c^2 + 4\chi_{n,c}$ can, at least in principle, be negative. This turns out to also not be a problem, since even when we only care about a small number of eigenfunctions, we can always compute more, say, $n + 100$, for which $\chi_{n+99,c}$ is positive.

4.2 Relative accuracy evaluation of the expansion coefficients of the eigenfunctions

Suppose that n is a non-negative integer. In Section 4.1, we expand each of the eigenfunctions $\psi_0, \psi_1, \ldots, \psi_n$ into a series of scaled Laguerre functions, and formulate an eigenproblem to solve for the expansion coefficients $\{\beta_k^{(j)}\}$ of ψ_j. We showed that, for the choice of basis functions described in Section 4.1, the number of required expansion coefficients N is not much larger than n. In fact, by Observation 4.3, the choice $N = 1.1n + |c| + 100$ is sufficient for all $c \in \mathbb{R}$. The coefficients are thus the solution to an eigenproblem involving a $(N + 1) \times (N + 1)$ five-diagonal matrix. Intuitively, one may suggest applying a standard eigensolver to solve for all eigenpairs of the five-diagonal matrix A. However, in this case, the eigenvalues and eigenvectors will only be evaluated to absolute precision, which turns out not to be sufficient for the relative accuracy evaluation of the spectrum of the integral operator $\mathcal{T}_c$. It turns out that, since the matrix is five-diagonal, the eigenvalues can be evaluated to relative precision and the eigenvectors can be evaluated to coordinate-wise relative precision. We derive the following algorithm for the relative accuracy evaluation of expansion coefficients of eigenfunctions $\{\psi_j\}_{j=0,1,\ldots,n}$ and the spectrum of $\mathcal{L}_c$:

1. Construct an $(N+1) \times (N+1)$ five-diagonal symmetric real matrix A whose entries are defined via (62), where a is chosen by formula (67) and Observation 4.2, and N is given by Observation 4.3.

2. Apply a regular symmetric five-diagonal eigenvalue solver to A to get a approximation of its eigenvalues $\chi_0, \chi_1, \ldots, \chi_N$ to absolute precision.

3. Apply the shifted inverse power method to A with an initial shift of $\chi_0, \chi_1, \ldots, \chi_n$, until convergence. This leads to an approximation of the expansion coefficients of $\{\psi_j\}_{j=0,1,\ldots,n}$ to coordinate-wise relative precision and the spectrum of $\mathcal{L}_c$ to relative precision.

Remark 4.6. For any $j \in \{0, 1, \ldots, n\}$, let $\tilde{\beta}^{(j)} = \left(\tilde{\beta}_0^{(j)}, \tilde{\beta}_1^{(j)}, \ldots, \tilde{\beta}_N^{(j)}\right) \in \mathbb{R}^{N+1}$ denote the true answer to the first $N+1$ coefficients of the expansion of ψ_j. Then each component of the approximation β_j produced by the shifted inverse power method in the third step of the algorithm has the following property, no matter how tiny the component is:

$$\frac{|\beta_k^{(j)} - \tilde{\beta}_k^{(j)}|}{|\tilde{\beta}_k^{(j)}|} < \epsilon, \ \forall k \in \{0, 1, \ldots, N\}, \tag{68}$$

where ϵ represents the machine epsilon (see [16] for more details). However with a regular eigensolver, one can only achieve

$$|\beta_k^{(j)} - \tilde{\beta}_k^{(j)}| < \epsilon, \ \forall k \in \{0, 1, \ldots, N\}, \text{ although } \frac{\|\beta^{(j)} - \tilde{\beta}^{(j)}\|_2}{\|\tilde{\beta}^{(j)}\|_2} < \epsilon. \tag{69}$$

In other words, the regular eigensolver can only achieve absolute precision for each coordinate of the eigenvectors, while the shifted inverse power method achieves relative precision.

Remark 4.7. The eigenvectors $\beta^{(n+1)}, \beta^{(n+2)}, \ldots, \beta^{(N)} \in \mathbb{R}^{N+1}$ are never used in our algorithm, since they are not sufficient for expanding $\psi_{n+1}, \psi_{n+2}, \ldots, \psi_N$, respectively. However, it's necessary to have them, otherwise we cannot solve for the $N+1$ coefficients in the expansion of ψ_j, for $j = 0, 1, \ldots, n$.

Remark 4.8. The first and second steps of the algorithm cost $\mathcal{O}(n)$ and $\mathcal{O}(n^2)$ operations, respectively. The shifted inverse power method is applied to n eigenpairs in the third step, and each iteration costs $\mathcal{O}(n)$ operations. Note that the initial guesses for the eigenvalues are correct to absolute precision, and the eigenvalues are well-separated (see Section 2.4). Considering the cubic convergence rate of the inverse power method, the convergence usually requires less than five iterations. Thus, the third step costs $\mathcal{O}(n^2)$ operations. So in total, the cost of the algorithm is $\mathcal{O}(n^2)$ operations.

4.3 Relative accuracy evaluation of the spectrum of the integral operator

In this subsection, we introduce an algorithm that evaluates $\mathcal{T}_c$'s eigenvalues $\lambda_0, \lambda_1, \ldots, \lambda_n$ to relative precision, using the expansion coefficients of the eigenfunctions computed from $\mathcal{L}_c$.

4.3.1 Evaluation of the first eigenvalue

By (32), we know that

$$\lambda_j = \frac{\int_0^\infty \mathrm{Ai}(x+y+c)\psi_j(y)\,\mathrm{d}y}{\psi_j(x)}. \tag{70}$$

We will show that, when the expansion coefficients of ψ_j are known to relative accuracy, for a particular choice of x, (70) can be used to evaluate λ_0 to relative accuracy.

Firstly, we discuss how to pick an optimal x, such that the evaluation is well-conditioned. Mathematically speaking, the choice of x makes no difference to the value of λ_0, but numerically, it's better to select x such that there's minimal cancellation in evaluating both $\psi_0(x)$ and $\int_0^\infty \mathrm{Ai}(x+y+c)\psi_0(y)\,\mathrm{d}y$. To achieve this, we notice that the Airy function is smooth and decaying on the right half-plane, and oscillatory on the left half-plane. So when c is non-negative, the integrand is decaying exponentially fast for any value of x, and $x = 0$ becomes a natural choice, since, for this value of x, the integrand is the largest. When c is negative, the integrand decays exponentially fast only when $x \geq -c$, so, in that case, $x = -c$ is similarly a natural choice. Therefore, we define x to be

$$x = \begin{cases} 0, & \text{if } c \geq 0 \\ -c, & \text{otherwise} \end{cases}. \tag{71}$$

We note that when $j = 0$, formula (70) is valid for any x chosen in this way. When $c \geq 0$, formula (108) shows that $\phi_0 \neq 0$. When $c < 0$, we have that $-c > 0$, so $\phi_0(-c) \neq 0$ by the Sturm oscillation theorem.

Once the value of x is chosen, we substitute the truncated expansion (64) of ψ_0 into (70), to get

$$\lambda_0 = \frac{\sum_{k=0}^N \beta_k^{(0)} \big(\int_0^\infty \mathrm{Ai}(x+y+c) h_k^a(y)\,\mathrm{d}y \big)}{\sum_{k=0}^N \beta_k^{(0)} h_k^a(x)}. \tag{72}$$

Note that the scaled Laguerre functions are easy to evaluate, and in the last section, we've already solved for $\{\beta_k^{(0)}\}_{k=0,1,\ldots,N}$ to relative accuracy. Thus, it's straightforward to compute the denominator of (72), and for our choice of x, it is evaluated without cancellation error. However, the computation of the numerator is more difficult due to the presence of integral $\int_0^\infty \mathrm{Ai}(x+y+c) h_k^a(y)\,\mathrm{d}y$. The integrand is highly oscillatory as k gets larger and c gets more negative, which implies that a plain quadrature method will be insufficient. Instead, we derive a five-term linear homogeneous recurrence relation for $\int_0^\infty \mathrm{Ai}(x+y+c) h_k^a(y)\,\mathrm{d}y$ (see Theorem 3.3), and by combining it with the shifted inverse power method, we manage to evaluate the integral to relative accuracy, for all values of $k = 0, 1, \ldots, N$. The main ideas of the algorithm are as follows.

For consistency, we use H_k^a, which is first defined in Theorem 3.3, to represent the integral $\int_0^\infty \mathrm{Ai}(x+y+c) h_k^a(y)\,\mathrm{d}y$. It follows that the variable s defined in (44) of Theorem 3.3 equals $x + c$ in our case. Clearly, the absolute value of H_k^a decays exponentially fast

as k increases, since the integrand becomes more and more oscillatory (See Theorem 2.5). The key point is that, it turns out that only one of the three linearly independent solutions to the five-term linear homogeneous recurrence relation satisfying (73) decays as $k \to \infty$. This implies that, by truncating the infinite matrix associated with the recurrence relation and evaluating the eigenvector corresponding to the zero eigenvalue, we can solve for H_k^a in a manner similar to Section 4.1. To put it more precisely, we first write out the recurrence relation in the form of a linear system:

$$B_{1,0}H_0^a + B_{1,1}H_1^a + B_{1,2}H_2^a + B_{1,3}H_3^a = 0 \tag{73}$$

$$B_{k-2,k}H_{k-2}^a + B_{k-1,k}H_{k-1}^a + B_{k,k}H_k^a + B_{k+1,k}H_{k+1}^a + B_{k+2,k}H_{k+2}^a = 0, \tag{74}$$

for $k = 2, 3, \ldots$, where $B_{k-2,k}, B_{k-1,k}, B_{k,k}, B_{k+1,k}, B_{k+2,k}$ are defined via the formulas

$$B_{k-2,k} = k - 1, \tag{75}$$

$$B_{k-1,k} = -(4k - 1 + a(x + c) - \frac{1}{4}a^3), \tag{76}$$

$$B_{k,k} = 6k + 3 + 2a(x + c) + \frac{1}{2}a^3, \tag{77}$$

$$B_{k,k+1} = -(4k + 5 + a(x + c) - \frac{1}{4}a^3), \tag{78}$$

$$B_{k,k+2} = k + 2, \tag{79}$$

for $k = 1, 2, \ldots$. Note that the first row of the infinite matrix B is all zeros. If we consider the eigenproblem for the infinite matrix B, by our observation, it must have an eigenvector corresponding to the zero eigenvalue, and the coordinates of the eigenvector decay exponentially fast. Therefore, if we want to evaluate the first $N + 1$ coordinates of the eigenvector with eigenvalue zero, we can replace the infinite matrix B with its its $(N' + 1) \times (N' + 1)$ upper left square submatrix, where $N' = \mathcal{O}(N)$ is sufficiently large, and apply an inverse power method (with shift zero) to B. The fact that there is only one decaying solution to the recurence relation which satisfies (73) means that this leads to an eigenvector $\{\tilde{H}_k^a\}_{k=0,1,\ldots,N'}$ whose first $n + 1$ coordinates match $\{H_k^a\}_{k=0,1,\ldots,N}$ to relative accuracy, up to some scalar factor.

Remark 4.9. To avoid division by zero, we set $B_{0,0}$ to be ϵ during computation, where ϵ is the smallest floating-point number.

Therefore, the last step is to normalize the eigenvector, such that the k-th coordinate equals H_k^a. This can be achieved by first computing H_0^a to relative precision, and multiplying every coordinate of the eigenvector by $H_0^a/\tilde{H}_0^a$. Note that, by our particular choice of x, the integrand of $H_0^a = \int_0^\infty \mathrm{Ai}(x + y + c)h_0^a(y)\,\mathrm{d}y$ is smooth and decays exponentially and monotonically. Thus, the evaluation can be done rapidly and accurately via quadrature.

Remark 4.10. Empirically, $N' = N + 40$ is a safe choice for the truncation of the infinite matrix B.

The first eigenvalue of the integral operator $\mathcal{T}_c$ can now be evaluated to relative precision by (72), using our computed expansion coefficients $\beta^{(0)}$ and the solution to the recurrence relation $\{H_k^a\}_{k=0,1,\ldots,N}$.

4.3.2 Evaluation of the rest of the eigenvalues

The standard way to overcome the obstacle for the numerical evaluation of small λ_j's is to compute all the ratios $\frac{\lambda_1}{\lambda_0}, \ldots, \frac{\lambda_n}{\lambda_{n-1}}$, and then evaluate the eigenvalue λ_j via the formula

$$\lambda_j = \lambda_0 \cdot \frac{\lambda_1}{\lambda_0} \cdot \cdots \cdot \frac{\lambda_j}{\lambda_{j-1}}, \tag{80}$$

where the ratio $\frac{\lambda_{n+1}}{\lambda_n}$ can be computed by Theorem 3.4:

$$\frac{\lambda_{n+1}}{\lambda_n} = \frac{\int_0^\infty \psi_n'(x)\psi_{n+1}(x)\,\mathrm{d}x}{\int_0^\infty \psi_n(x)\psi_{n+1}'(x)\,\mathrm{d}x}, \tag{81}$$

(see Section 10.2 in [17]).

Clearly, the computation can be done spectrally: for example, one can evaluate the numerator of (81) by first computing the expansion of the derivative of ψ_n via Corollary 2.3, then computing the inner product of the two series expansions of ψ_n' and ψ_{n+1} by orthogonality of the basis functions. The denominator is symmetric to the numerator, and can be computed in essentially the same way. Therefore, it takes $\mathcal{O}(N)$ operations to compute $\frac{\lambda_{n+1}}{\lambda_n}$, and takes $\mathcal{O}(nN)$ operations in total to compute λ_j for $j = 1, 2, \ldots, n$. Recalling that $N = 1.1n + |c| + 100$, we see that the cost is $\mathcal{O}(n^2 + |c|n)$.

Remark 4.11. One may also compute the expansion of the derivative of ψ_n by applying a differentiation matrix (see 14) to the expansion coefficients $\beta^{(n)}$ of ψ_n. However, this will cost $\mathcal{O}(N^2)$ operations for each differentiation, which makes the total cost be $\mathcal{O}(nN^2)$ operations.

5 Numerical Experiments

We implemented our algorithm in FORTRAN 77, and compiled it using Lahey/Fujitsu Fortran 95 Express, Release L6.20e. For the timing experiments, the Fortran codes were compiled using the Intel Fortran Compiler, version 2021.2.0, with the `-fast` flag. We conducted all experiments on a ThinkPad laptop, with 16GB of RAM and an Intel Core i7-10510U CPU.

5.1 Computation of the eigenfunctions and spectra

In this section, we report the plots of the eigenfunctions and spectra for different values of c and n (see Figures 1, 2), and the corresponding computation times (see Table 1). We normalize the eigenfunctions $\phi_{n,c}$ by requiring that $\phi_{n,c}(0) > 0$ (recall that $\phi_{n,c}(0) \neq 0$, see (108)). In addition, we illustrate the importance of selecting the optimal scaling factor of the scaled Laguerre functions in Figure 3.

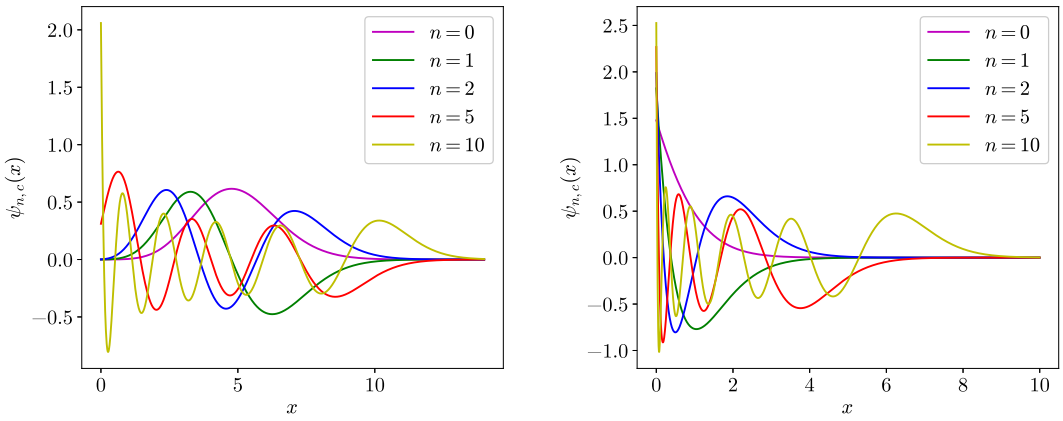

(a) $c = -10$ (b) $c = 0$

(c) $c = 10$ (d) $c = 20$

Figure 1: **Eigenfunctions of different orders with different parameters** c.

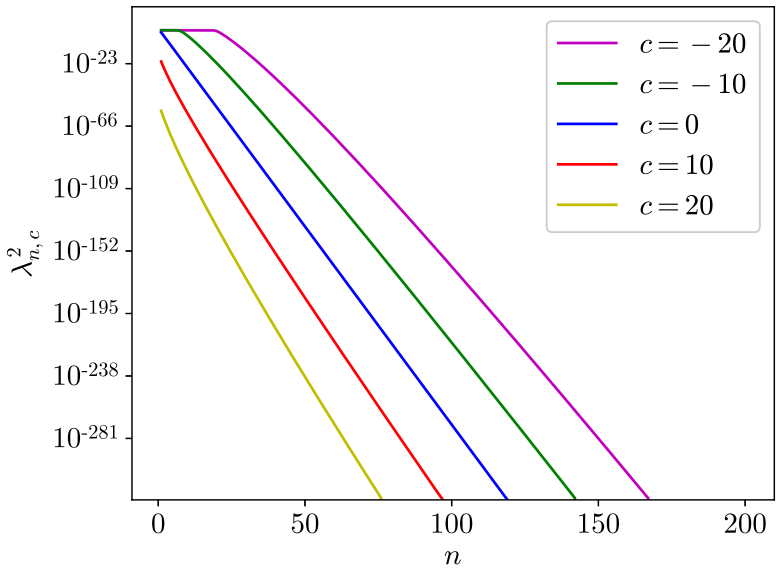

Figure 2: **Square of the spectra of the Airy integral operator with different parameters** c. This correspond to the spectra of the integral operator with the kernel $K_{\mathrm{Ai}}(x, y)$ (see (33), (82)). Note that the leading eigenvalues converge to 1 as $c \to -\infty$.

c	n	N	Time
20	50	175	2.10×10^{-3} secs
	100	230	3.64×10^{-3} secs
	200	340	8.76×10^{-3} secs
	400	560	3.35×10^{-2} secs
0	50	155	3.36×10^{-3} secs
	100	210	4.93×10^{-3} secs
	200	320	9.75×10^{-3} secs
	400	540	3.17×10^{-2} secs
-20	50	175	4.32×10^{-3} secs
	100	230	5.64×10^{-3} secs
	200	340	1.14×10^{-2} secs
	400	560	3.37×10^{-2} secs

Table 1: **The computation time of the eigenfunctions and spectra of the integral operator for different value of** c **and** n. The value of N is determined by Observation (4.3). The time cost is of order $\mathcal{O}(N^2)$ as N increases. Note that in our current implementation, we use the naive inverse power method instead of the shifted version. The computation times will improve further after we switch to the shifted inverse power method.

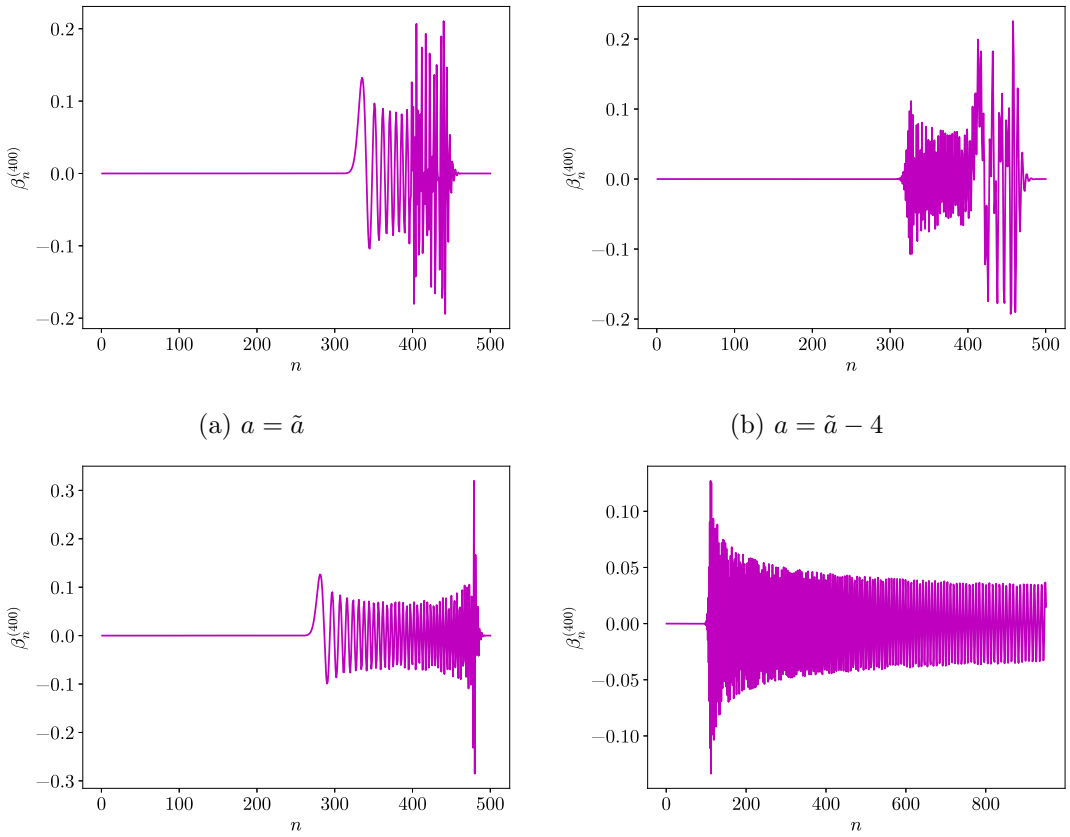

(a) $a = \tilde{a}$ (b) $a = \tilde{a} - 4$

(c) $a = \tilde{a} + 4$ (d) $a = 1$

Figure 3: **Expansion coefficients of $\psi_{n,c}$ in the basis of scaled Laguerre functions with different scaling factors a, where $n = 400$, $c = 10$.** Note that the optimal scaling factor $\tilde{a} \approx 20.62$, and is selected by formula (67). It's clear that our basis functions becomes optimal when $a = \tilde{a}$. Figure (d) shows that the unscaled Laguerre functions are unsuitable for approximating the eigenfunctions of the Airy integral operator.

5.2 Computation of the Tracy-Widom distribution

The cumulative distribution function (CDF) of the large matrix limit of the Gaussian unitary ensemble (GUE), scaled for the fluctuations at the soft edge, can be written in the following determinantal representation:

$$F_2(s) = \det(I - K_{\mathrm{Ai}}|_{L^2[s,\infty)}), \tag{82}$$

where $K_{\mathrm{Ai}}|_{L^2[s,\infty)}$ denotes the integral operator on $L^2[s,\infty)$ with kernel

$$K_{Ai}(x,y) = \frac{\mathrm{Ai}(x)\mathrm{Ai}'(y) - \mathrm{Ai}'(x)\mathrm{Ai}(y)}{x-y}. \tag{83}$$

It's shown in [22] that

$$K_{Ai}(x,y) = \int_s^\infty \mathrm{Ai}(x+z-s)\mathrm{Ai}(z+y-s)\,\mathrm{d}z, \tag{84}$$

from which it follows that, for any $f \in L^2[s,\infty)$,

$$\int_s^\infty K_{Ai}(x,y)f(y)\,\mathrm{d}y = \mathcal{G}_s^2[f], \tag{85}$$

where $\mathcal{G}_s$ is the Airy integral operator defined in Section 2.3, whose eigenvalues are $\mu_{0,s}, \mu_{1,s}, \dots$.

Therefore,

$$F_2(s) = \det(I - K_{Ai}|_{L^2(s,\infty)}) = \prod_{i=0}^\infty (1-\mu_{i,s}^2) = \prod_{i=0}^\infty (1-\lambda_{i,s}^2), \tag{86}$$

where λ_i is the eigenvalues of the associated Airy integral operator $\mathcal{T}_s$ (see Section 2.3), and where the last equality holds because $\mu_{i,s} = \lambda_{i,s}$ (see formula (33)).

Correspondingly, the probability density function (PDF) of the Tracy-Widom distribution function can be written as

$$\begin{aligned}\frac{d}{ds}F_2(s) &= \sum_{j=0}^\infty \Big(-2\lambda_{j,s}\frac{\partial \lambda_{j,s}}{\partial s} \prod_{i=0, i\neq j}^\infty (1-\lambda_{i,s}^2)\Big) \\ &= \sum_{j=0}^\infty \Big(\lambda_{j,s}^2 \big(\psi_{j,s}(0)\big)^2 \prod_{i=0, i\neq j}^\infty (1-\lambda_{i,s}^2)\Big),\end{aligned} \tag{87}$$

where $\psi_{j,s}$ is the j-th eigenfunction of $\mathcal{T}_s$. The last equality holds due to the identity

$$\frac{\partial \lambda_{n,s}}{\partial s} = -\frac{1}{2}\lambda_{n,s}\big(\psi_{n,s}(0)\big)^2, \tag{88}$$

(see Theorem 6.1).

We report the computation time and the numerical errors of the PDF and CDF in Tables 2, 3. The errors are computed using the table provided in [19].

s	n	N	Time	Relative error	Absolute error	$\frac{d}{ds}F_2(s)$
50	30	40	2.36×10^{-4} secs	1.60×10^{-15}	2.38×10^{-223}	1.48437×10^{-208}
25	30	40	2.23×10^{-4} secs	1.98×10^{-14}	1.30×10^{-89}	6.56096×10^{-76}
10	20	30	1.88×10^{-4} secs	2.16×10^{-14}	4.10×10^{-35}	1.90064×10^{-21}
5	20	30	2.09×10^{-4} secs	2.59×10^{-14}	6.53×10^{-23}	2.52105×10^{-9}
2	20	30	2.26×10^{-4} secs	7.26×10^{-14}	2.75×10^{-17}	3.79199×10^{-4}
0	30	40	1.32×10^{-3} secs	3.11×10^{-15}	2.08×10^{-16}	6.69753×10^{-2}
-2	30	40	1.54×10^{-3} secs	1.51×10^{-15}	6.66×10^{-16}	4.41382×10^{-1}
-5	40	50	1.59×10^{-3} secs	6.63×10^{-13}	8.89×10^{-17}	1.34039×10^{-4}
-10	50	60	1.24×10^{-3} secs	3.84×10^{-4}	4.05×10^{-39}	1.05359×10^{-35}
-20	100	150	2.80×10^{-3} secs	7.95×10^{86}	1.41×10^{-199}	1.77193×10^{-288}

Table 2: **The evaluation of the probability density function**. The actual values of $\frac{d}{ds}F_2(s)$ are rounded to 6 significant digits.

s	n	N	Time	Relative error	Absolute error	$F_2(s)$
50	30	40	2.36×10^{-4} secs	0	0	1.00000×10^{0}
25	30	40	2.23×10^{-4} secs	0	0	1.00000×10^{0}
10	20	30	1.88×10^{-4} secs	0	0	1.00000×10^{0}
5	20	30	2.09×10^{-4} secs	0	0	1.00000×10^{0}
2	20	30	2.26×10^{-4} secs	0	0	9.99888×10^{-1}
0	30	40	1.32×10^{-3} secs	1.15×10^{-16}	1.11×10^{-16}	9.69373×10^{-1}
-2	30	40	1.54×10^{-3} secs	1.88×10^{-15}	7.77×10^{-16}	4.41322×10^{-1}
-5	40	50	1.59×10^{-3} secs	1.27×10^{-12}	2.72×10^{-17}	2.13600×10^{-5}
-10	50	60	1.24×10^{-3} secs	4.66×10^{-4}	1.96×10^{-40}	4.21226×10^{-37}
-20	100	150	2.80×10^{-3} secs	1.69×10^{87}	2.99×10^{-203}	1.77182×10^{-290}

Table 3: **The evaluation of the cumulative distribution function**. The actual values of $F_2(s)$ are rounded to 6 significant digits.

Remark 5.1. The computation times of the PDF and the CDF are almost identical (see Tables 2, 3), since the cost of evaluating formulas (86) and (87) is negligible compared with the cost of computing the spectrum of the integral operator.

Observation 5.2. Our algorithm evaluates the PDF and CDF to relative accuracy when $s \geq -5$. The algorithm only evaluates the left tail of the Tracy-Widom distribution (when $s < -5$) to absolute precision, since the leading eigenvalues of the integral operator with the kernel K_{Ai} are close to 1 when $s < -5$, which leads to catastrophic cancellation in the computation of the PDF and CDF (see formulas (86), (87)). The numerical apparatus

for evaluating the left tail of the distribution to relative precision is almost identical (see Section 7.1).

6 Miscellaneous properties

In this section, we describe miscellaneous properties of the eigenfunctions $\psi_{n,c}$ of the operators $\mathcal{T}_c$ and $\mathcal{L}_c$, as well as properties of the eigenvalues $\chi_{n,c}$ of the differential operator $\mathcal{L}_c$, and $\lambda_{n,c}$ of the integral operators $\mathcal{T}_c$, $\mathcal{G}_c$.

6.1 Derivative of $\lambda_{n,c}$ with respect to c

Theorem 6.1. *For all real c and non-negative integers n,*

$$\frac{\partial \lambda_{n,c}}{\partial c} = -\frac{1}{2}\lambda_{n,c}\big(\psi_{n,c}(0)\big)^2. \tag{89}$$

Proof. Given two real numbers a, c, define $\epsilon = \frac{c-a}{2}$. By (32),

$$\lambda_{n,c}\psi_{n,c}(x)\psi_{n,a}(x+\epsilon) = \psi_{n,a}(x+\epsilon)\int_0^\infty \mathrm{Ai}(x+y+c)\psi_{n,c}(y)\,\mathrm{d}y. \tag{90}$$

We integrate both sides of (90) over the interval $[0,\infty)$ with respect to x to obtain

$$\begin{aligned}
&\lambda_{n,c}\int_0^\infty \psi_{n,c}(x)\psi_{n,a}(x+\epsilon)\,\mathrm{d}x = \int_0^\infty \psi_{n,c}(y)\int_0^\infty \mathrm{Ai}(x+y+c)\psi_{n,a}(x+\epsilon)\,\mathrm{d}x\,\mathrm{d}y\\
&= \int_0^\infty \psi_{n,c}(y)\int_\epsilon^\infty \mathrm{Ai}(y+\epsilon+s+a)\psi_{n,a}(s)\,\mathrm{d}s\,\mathrm{d}y\\
&= \int_0^\infty \psi_{n,c}(y)\Big(\lambda_{n,a}\psi_{n,a}(y+\epsilon) + \int_\epsilon^0 \mathrm{Ai}(y+\epsilon+s+a)\psi_{n,a}(s)\,\mathrm{d}s\Big)\,\mathrm{d}y,
\end{aligned} \tag{91}$$

where the change of variable $s = x+\epsilon$ is applied in (91). After rearranging the terms, we have

$$(\lambda_{n,c}-\lambda_{n,a})\int_0^\infty \psi_{n,c}(x)\psi_{n,a}(x+\epsilon)\,\mathrm{d}x = \int_0^\infty \psi_{n,c}(y)\Big(\int_\epsilon^0 \mathrm{Ai}(y+\epsilon+s+a)\psi_{n,a}(s)\,\mathrm{d}s\Big)\,\mathrm{d}y. \tag{92}$$

Then we divide both sides by 2ϵ and take the limit $2\epsilon \to 0$. The left side of (92) becomes

$$\begin{aligned}
&\lim_{2\epsilon\to 0}\frac{\lambda_{n,c}-\lambda_{n,a}}{2\epsilon}\int_0^\infty \psi_{n,c}(x)\psi_{n,a}(x+\epsilon)\,\mathrm{d}x = \frac{\partial\lambda_{n,c}}{\partial c}\lim_{a\to c}\int_0^\infty \psi_{n,c}(x)\psi_{n,a}(x+\frac{c-a}{2})\,\mathrm{d}x\\
&= \frac{\partial\lambda_{n,c}}{\partial c}\|\psi_{n,c}\|_2^2\\
&= \frac{\partial\lambda_{n,c}}{\partial c}.
\end{aligned} \tag{93}$$

The right side of (92) becomes

$$\begin{aligned}
&\lim_{2\epsilon\to 0}\frac{1}{2\epsilon}\int_0^\infty \psi_{n,c}(y)\Big(\int_\epsilon^0 \mathrm{Ai}(y+\epsilon+s+a)\psi_{n,a}(s)\,\mathrm{d}s\Big)\,\mathrm{d}y\\
&= -\frac{1}{2}\psi_{n,c}(0)\lim_{a\to c}\int_0^\infty \mathrm{Ai}\Big(y+\frac{c+a}{2}\Big)\psi_{n,c}(y)\,\mathrm{d}y\\
&= -\frac{1}{2}\lambda_{n,c}\big(\psi_{n,c}(0)\big)^2.
\end{aligned} \tag{94}$$

Finally, by combining (92), (93), and (94),

$$\frac{\partial \lambda_{n,c}}{\partial c} = -\frac{1}{2}\lambda_{n,c}\big(\psi_{n,c}(0)\big)^2. \tag{95}$$

■

The following corollaries are immediate consequences of the preceding one.

Corollary 6.2. *For all real c and non-negative integers m, n,*

$$\frac{\partial}{\partial c}\Big(\frac{\lambda_{m,c}}{\lambda_{n,c}}\Big) = \frac{\lambda_{m,c}\Big((\psi_{n,c}(0))^2 - (\psi_{m,c}(0))^2\Big)}{2\lambda_{n,c}}. \tag{96}$$

Corollary 6.3. *For all real c and non-negative integers n,*

$$\frac{\partial \lambda_{n,c}^2}{\partial c} = -\lambda_{n,c}^2\big(\psi_{n,c}(0)\big)^2. \tag{97}$$

6.2 Derivative of $\chi_{n,c}$ with respect to c

Theorem 6.4. *For all real number c and non-negative integers n,*

$$\frac{\partial \chi_{n,c}}{\partial c} = \int_0^\infty x\big(\psi_{n,c}(x)\big)^2 \,\mathrm{d}x. \tag{98}$$

Proof. Due to (36),

$$\frac{d}{dx}\Big(x\frac{d}{dx}\psi_{n,c}\Big) - (x^2 + cx - \chi_n)\psi_{n,c} = 0. \tag{99}$$

With the infinitesimal changes $c = c + h$, it follows that $\chi_n = \chi_n + \epsilon$, $\psi_{n,c}(x) = \psi_{n,c}(x) + \delta(x)$. Therefore, (99) becomes

$$\frac{d}{dx}\Big(x\frac{d}{dx}(\psi_{n,c} + \delta)\Big) - (x^2 + (c+h)x - (\chi_n + \epsilon))(\psi_{n,c} + \delta) = 0. \tag{100}$$

After subtracting (99) from (100) and discarding infinitesimals of second order or greater, (100) becomes

$$\mathcal{L}_c[\delta](x) + (hx - \epsilon)\psi_{n,c}(x) = 0, \tag{101}$$

where $\mathcal{L}_c$ is defined by (35). Then we multiply both sides of (101) by $\frac{\psi_{n,c}(x)}{h}$ and integrate both sides over the interval $[0, \infty)$, which gives us

$$\frac{1}{h}\int_0^\infty \mathcal{L}_c[\delta](x)\psi_{n,c}(x)\,\mathrm{d}x + \int_0^\infty x\big(\psi_{n,c}(x)\big)^2\,\mathrm{d}x - \frac{\epsilon}{h}\int_0^\infty \big(\psi_{n,c}(x)\big)^2 = 0. \tag{102}$$

Due to the self-adjointness of $\mathcal{L}_c$,

$$\frac{1}{h}\int_0^\infty \mathcal{L}_c[\delta](x)\psi_{n,c}(x)\,\mathrm{d}x = \frac{1}{h}\int_0^\infty \delta(x)\mathcal{L}_c[\psi_{n,c}](x)\,\mathrm{d}x = 0. \tag{103}$$

By (103) and the fact that $\|\psi_{n,c}\|_2^2 = 1$, in the appropriate limit, (102) becomes

$$\frac{\partial \chi_{n,c}}{\partial c} = \int_0^\infty x\big(\psi_{n,c}(x)\big)^2\,\mathrm{d}x. \tag{104}$$

■

6.3 Recurrence relations involving the derivatives of the eigenfunctions

Theorem 6.5. *For all real number c, non-negative integers n, and $x \in [0, \infty)$,*

$$\begin{aligned} &- k(k-1)\psi_{n,c}^{(k-2)}(x) - 5(c+2x)\psi_{n,c}^{(k-1)}(x) + \left(\chi_{n,c} - cx - x^2\right)\psi_{n,c}^{(k)}(x) \\ &+ (k+1)\psi_{n,c}^{(k+1)}(x) + x\psi_{n,c}^{(k+2)}(x) = 0, \end{aligned} \tag{105}$$

for all $k \geq 2$. Furthermore,

$$-(c+2x)\psi_{n,c}(x) + (\chi_{n,c} - cx - x^2)\psi_{n,c}'(x) + 2\psi_{n,c}''(x) + x\psi_{n,c}^{(3)}(x) = 0. \tag{106}$$

In particular, for all positive real c, non-negative integers n,

$$\chi_{n,c}\psi_{n,c}(0) + \psi_{n,c}'(0) = 0, \tag{107}$$

$$\psi_{n,c}(0) \neq 0. \tag{108}$$

Proof. The identities (105) and (106) are immediately obtained by repeated differentiation of (36).
The identity (107) is proved by plugging $x = 0$ into (36).
Finally, the identity (108) can be easily verified via proof by contradiction. ■

Remark 6.1. We can compute the initial conditions $\psi_{n,c}(x)$ and $\psi_{n,c}'(x)$ by evaluating the truncated expansion (64) and its first derivative in $\mathcal{O}(N)$ operations, where N represents the size of the matrix. The higher derivatives can then be calculated via identities (36), (106) and (105) in $\mathcal{O}(1)$ operations. This theorem is useful for computing the Taylor expansion of $\psi_{n,c}$ at a given point x.

Corollary 6.6. *For all positive real c, non-negative integers m, n,*

$$(\chi_{m,c} - \chi_{n,c})\psi_{m,c}(0)\psi_{n,c}(0) + \psi_{m,c}'(0)\psi_{n,c}(0) - \psi_{m,c}(0)\psi_{n,c}'(0) = 0. \tag{109}$$

Proof. The corollary follows directly from the equation (107). ■

6.4 Expansion in terms of the eigenfunctions

Given a real number c, the functions $\psi_{0,c}, \psi_{1,c}, \ldots$ are a complete orthonormal basis in $L^2[0, \infty)$. Therefore, given $f \in L^2[0, \infty)$, we refer the expansion of f in the basis $\{\psi_{n,c}\}$ as the $\psi_{n,c}$ expansion. In this subsection, we'll provide identities that give the $\psi_{n,c}$ expansion of the derivatives of a $\psi_{n,c}$ expansion, a $\psi_{n,c}$ expansion multiplied by x, as well as a $\psi_{n,c}$ expansion differentiated with respect to c.

Theorem 6.7. *For any real c, non-negative integers m, n,*

$$\int_0^\infty \psi_n'(x)\psi_m(x)\,\mathrm{d}x = -\frac{\lambda_m}{\lambda_n + \lambda_m}\psi_n(0)\psi_m(0). \tag{110}$$

If $m \neq n$, then

$$\int_0^\infty \psi_n''(x)\psi_m(x)\,\mathrm{d}x = \frac{\lambda_m}{\lambda_m - \lambda_n}\Big(\psi_n'(0)\psi_m(0) - \psi_n(0)\psi_m'(0)\Big), \tag{111}$$

$$\int_0^\infty x\psi_n(x)\psi_m(x)\,\mathrm{d}x = \frac{\lambda_n\lambda_m}{\lambda_m^2 - \lambda_n^2}\Big(\psi_n'(0)\psi_m(0) - \psi_n(0)\psi_m'(0)\Big), \tag{112}$$

$$\int_0^\infty \frac{\partial\psi_n}{\partial c}(x)\psi_{m,c}(x)\,\mathrm{d}x = \frac{\lambda_n\lambda_m}{\lambda_m^2 - \lambda_n^2}\psi_m(0)\psi_n(0), \tag{113}$$

where $\psi_m, \psi_n, \lambda_m, \lambda_n$ denote the eigenfunctions and eigenvalues of the Airy integral operator with parameter c.

Proof. To prove (110), we start with the identity

$$\lambda_n \int_0^\infty \psi_n'(x)\psi_m(x)\,\mathrm{d}x = \int_0^\infty \Big(\int_0^\infty \frac{d}{dx}\mathrm{Ai}(x+y+c)\psi_n(y)\,\mathrm{d}y\Big)\psi_m(x)\,\mathrm{d}x. \tag{114}$$

Note that

$$\frac{d}{dx}\mathrm{Ai}(x+y+c) = \frac{d}{dy}\mathrm{Ai}(x+y+c). \tag{115}$$

Therefore, the above calculation (114) can be repeated with m and n exchanged, yielding the identity

$$\begin{aligned}\lambda_m \int_0^\infty \psi_m'(x)\psi_n(x)\,\mathrm{d}x &= \int_0^\infty \Big(\int_0^\infty \frac{d}{dx}\mathrm{Ai}(x+y+c)\psi_m(y)\,\mathrm{d}y\Big)\psi_n(x)\,\mathrm{d}x \\ &= \int_0^\infty \Big(\int_0^\infty \frac{d}{dy}\mathrm{Ai}(y+x+c)\psi_n(x)\,\mathrm{d}x\Big)\psi_m(y)\,\mathrm{d}y\end{aligned} \tag{116}$$

By combining (114) and (116), we get

$$\int_0^\infty \psi_n'(x)\psi_m(x)\,\mathrm{d}x = \frac{\lambda_m}{\lambda_n}\int_0^\infty \psi_m'(x)\psi_n(x)\,\mathrm{d}x. \tag{117}$$

On the other hand, integrating the right side of (117) by parts and rearranging the terms gives (110).

The equation (111) is proved in a similar way. By combining (3) and (32), we derive the following identity:

$$\lambda_n\psi_n''(x) = \int_0^\infty (x+y+c)\mathrm{Ai}(x+y+c)\psi_n(y)\,\mathrm{d}y. \tag{118}$$

By repeating the same procedure (114)-(117), we get

$$\int_0^\infty \psi_n''(x)\psi_m(x)\,\mathrm{d}x = \frac{\lambda_m}{\lambda_n}\int_0^\infty \psi_m''(x)\psi_n(x)\,\mathrm{d}x. \tag{119}$$

Integrating the right side of (119) by parts twice and rearranging the terms gives (111).

To prove (112), first note that by combining (118) and (32), we get

$$\lambda_n\Big(\psi_n''(x)-(x+c)\psi_n(x)\Big)=\int_0^\infty y\mathrm{Ai}(x+y+c)\psi_n(y)\,\mathrm{d}y. \tag{120}$$

Project both sides of (120) on $\psi_m(x)$, we have

$$\begin{aligned}&\lambda_n\int_0^\infty\Big(\psi_n''(x)-(x+c)\psi_n(x)\Big)\psi_m(x)\,\mathrm{d}x=\int_0^\infty\int_0^\infty y\mathrm{Ai}(x+y+c)\psi_n(y)\,\mathrm{d}y\,\psi_m(x)\,\mathrm{d}x\\&=\int_0^\infty y\psi_n(y)\int_0^\infty\mathrm{Ai}(y+x+c)\psi_m(x)\,\mathrm{d}x\;\mathrm{d}y\\&=\lambda_m\int_0^\infty y\psi_n(y)\psi_m(y)\,\mathrm{d}y\end{aligned} \tag{121}$$

Therefore, (121) becomes

$$(\lambda_m+\lambda_n)\int_0^\infty x\psi_n(x)\psi_m(x)\,\mathrm{d}x=\lambda_n\int_0^\infty\Big(\psi_n''(x)-c\psi_n(x)\Big)\psi_m(x)\,\mathrm{d}x. \tag{122}$$

By combining the orthogonality of ψ_n, (111) and (89), we proved (112).

To prove (113), we take the derivative with respect to c of both sides of (32), yielding the identity

$$\frac{\partial\lambda_n}{\partial c}\psi_n(x)+\lambda_n\frac{\partial\psi_n}{\partial c}(x)=\int_0^\infty\Big(\frac{d}{dc}\mathrm{Ai}(x+y+c)\psi_n(y)+\mathrm{Ai}(x+y+c)\frac{\partial\psi_n}{\partial c}(y)\Big)\,\mathrm{d}y. \tag{123}$$

Project both sides of (123) on $\psi_m(x)$, by (32), we get

$$\begin{aligned}&\lambda_n\int_0^\infty\frac{\partial\psi_n}{\partial c}(x)\psi_m(x)\,\mathrm{d}x\\&=\int_0^\infty\Big(\int_0^\infty\frac{d}{dc}\mathrm{Ai}(x+y+c)\psi_n(y)\,\mathrm{d}y\Big)\psi_m(x)\,\mathrm{d}x+\lambda_m\int_0^\infty\frac{\partial\psi_n}{\partial c}(y)\psi_m(y)\,\mathrm{d}y.\end{aligned} \tag{124}$$

Since

$$\frac{d}{dx}\mathrm{Ai}(x+y+c)=\frac{d}{dc}\mathrm{Ai}(x+y+c), \tag{125}$$

and (32) implies

$$\lambda_n\psi_n'(x)=\int_0^\infty\frac{d}{dc}\mathrm{Ai}(x+y+c)\psi_n(y)\,\mathrm{d}y, \tag{126}$$

we have

$$\int_0^\infty\Big(\int_0^\infty\frac{d}{dc}\mathrm{Ai}(x+y+c)\psi_n(y)\,\mathrm{d}y\Big)\psi_m(x)\,\mathrm{d}x=\lambda_n\int_0^\infty\psi_n'(x)\psi_m(x)\,\mathrm{d}x. \tag{127}$$

Finally, by combining (110), (124) and (127), we proved (113). ■

7 Conclusions and Generalizations

In this report, we present a numerical algorithm for rapidly evaluating the eigendecomposition of the integral operator $\mathcal{T}_c$ (equivalently, $\mathcal{G}_c$), defined in (30). Our method computes the eigenvalues $\lambda_{j,c}$ of $\mathcal{T}_c$ to full relative accuracy, and computes the eigenfunctions $\psi_{j,c}$ of $\mathcal{T}_c$ and $\mathcal{L}_c$ in the form of an expansion (58) in scaled Laguerre functions, where the expansion coefficients are also computed to full relative accuracy. In Section 5.2, we observe that this algorithm can be used to rapidly evaluate the Tracy-Widom CDF $F_2(s)$ and PDF $\frac{d}{ds}F_2(s)$ everywhere to full absolute precision, and in the right tail to full relative precision. These results can be generalized in several directions, which we describe below.

7.1 Evaluation of the Tracy-Widom distribution to relative accuracy in the left tail

It's known that the eigenvalues $\lambda_{j,s}$ of $\mathcal{G}_s$ converge to 1 as $s \to -\infty$ (see, for example, [22]). As a result, both the CDF $F_2(s)$, given by formula (86), and the PDF $\frac{d}{ds}F_2(s)$, given by formula (87), approach zero as $s \to -\infty$. Since this decay is the result of cancellation between the eigenvalues and 1 in the evaluation of $1-\lambda_{j,s}^2$, it's clear that the CDF and PDF can both be evaluated only to absolute precision in the left tail, even if the eigenvalues are computed to full relative precision. This issue is resolved by considering the "complement" integral operator to the operator $K_{\mathrm{Ai}}|_{L^2[s,\infty)}$, with eigenvalues $\widetilde{\lambda}_{j,s}^2 = 1 - \lambda_{j,s}^2$. This integral operator is the square of an integral operator $\widetilde{\mathcal{G}}_s$, which can be shown to commute with a differential operator $\widetilde{\mathcal{L}}_s$. The eigenvalues $\widetilde{\lambda}_{j,s}$ can be computed to relative accuracy from the eigenfunctions of $\widetilde{\mathcal{L}}_s$, which means that the quantities $1 - \lambda_{j,s}^2$ can be computed to relative accuracy. Thus, in this fashion, $F_2(s)$ and $\frac{d}{ds}F_2(s)$ are computable by (86) and (87) to full relative accuracy in the left tail.

7.2 Distribution of the kth largest eigenvalue

The cumulative distribution function for the kth largest eigenvalue of the GUE is given by the formula

$$F_2(k,s) = \sum_{j=0}^{k-1} \frac{(-1)^j}{j!} \frac{d^j}{dz^j} \det(I - zK_{\mathrm{Ai}}|_{L^2[s,\infty)})\Big|_{z=1}, \tag{128}$$

where $K_{\mathrm{Ai}}|_{L^2[s,\infty)}$ is defined by formula (84) (see, for example, [2]). Since

$$\det(I - zK_{\mathrm{Ai}}|_{L^2[s,\infty)}) = \prod_{i=0}^{\infty}(1 - z\lambda_{i,s}^2), \tag{129}$$

where $\lambda_{i,s}$ is the ith eigenvalue of $\mathcal{G}_s$ (see formula (29)), a straightforward application of the product rule allows $F_2(k,s)$ to be computed from the spectrum of $\mathcal{G}_s$. Likewise, $\frac{d}{ds}F_2(k,s)$ can be computed from the values $\lambda_{i,s}$ and $\frac{\partial}{\partial s}\lambda_{i,s}$ along the same lines as Section 5.2. Thus, both the CDF $F_2(k,s)$ and the PDF $\frac{d}{ds}F_2(k,s)$ can be computed to absolute precision everywhere, and since the partials $\frac{\partial}{\partial s}\lambda_{i,s}$ are known to full relative precision, the PDF can be computed to full relative precision in the right tail.

8 Acknowledgements

We sincerely thank Jeremy Quastel for his helpful advice and informative conversations. The first author would like to thank Zhenkun Shen and Qiaoling Gu for their endless support, and he is fortunate, grateful, and proud of being their child.

References

[1] Abramowitz, M., and I. A. Stegun. *Handbook of Mathematical Functions With Formulas, Graphs, and Mathematical Tables.* Washington: U.S. Govt. Print. Off., 1964.

[2] Bornemann, F. "On the Numerical Evaluation of Distributions in Random Matrix Theory: A Review." *Markov Processes Relat. Fields* 16.4 (2010): 803–866.

[3] Bornemann, F. "On the numerical evaluation of Fredholm determinants." *Math. Comput* 79.270 (2010): 871–915.

[4] Bouchaud, J. P., M. Potters. "Financial Applications of Random Matrix Theory: a short review." *Handbook on Random Matrix Theory.* Oxford University Press, 2009.

[5] Caspera, W. R., F. A. Gruünbaumb, M. Yakimova, and I. Zurriánc. "Reflective prolate-spheroidal operators and the KP/KdV equations." *PNAS* 116.37 (2019): 18310–18315.

[6] Chiani M. "Distribution of the largest eigenvalue for real Wishart and Gaussian random matrices and a simple approximation for the TracyWidom distribution." *J. Multivar. Anal.* 129 (2014): 69–81.

[7] Couillet, R. and M. Debbah. *Random Matrix Methods for Wireless Communications.* Cambridge University Press, 2011.

[8] Dieng, M. "Distribution Functions for Edge Eigenvalues in Orthogonal and Symplectic Ensembles: Painlevé Representations.", PhD thesis, University of Davis. e-print: arXiv:math/0506586v2, 2005.

[9] Edelman, A. and N.R. Rao. "Random matrix theory." *Acta Numer.* 14 (2005): 233–297.

[10] Edelman, A. and P.O. Persson. "Numerical methods for eigenvalue distributions of random matrices." arXiv:math-ph/0501068, 2005.

[11] Forrester, P.J. "The spectrum edge of random matrix ensembles." *Nuclear Phys. B* 402.3 (1993): 709–728.

[12] Guhr, T., A. MüllerGroeling, and H. A. Weidenüller. "Random-matrix theories in quantum physics: common concepts." *Phys. Rep.* 299.4-6 (1998): 189–425.

[13] Karoui, A., I. Mehrzi, and T. Moumni. "Eigenfunctions of the Airy's integral transform: Properties, numerical computations and asymptotic behaviors." *J. Math. Anal. Appl.* 389.2 (2012):989–1005.

[14] Lederman, R.R. "On the Analytical and Numerical Properties of the Truncated Laplace Transform." *Technical Report*YALEU/DCS/TR-1490 (2014)

[15] Mehta, M. L. *Random matrices.* 3rd ed, Elsevier 2004.

[16] Osipov, A. "Evaluation of small elements of the eigenvectors of certain symmetric tridiagonal matrices with high relative accuracy." *Appl. Comput. Harmon. Anal.* 43.2 (2017): 173–211.

[17] Osipov, A., V. Rokhlin, and H. Xiao. *Prolate Spheroidal Wave Functions of Order Zero - Mathematical Tools for Bandlimited Approximation.* Springer, 2013.

[18] Paul, D. and A. Aue. "Random matrix theory in statistics: A review." *J. Stat. Plan. Inference* 150 (2014): 1–29.

[19] Prähofer, M. "Tables to: Exact scaling functions for one-dimensional stationary KPZ growth." `http://www-m5.ma.tum.de/KPZ/`, 2003.

[20] Schwarz, H. R. "Tridiagonalization of a symetric band matrix." *Numer. Math.* 12.4 (1968): 231–241.

[21] Slepian, D. and H. O. Pollak. "Prolate Spheroidal Wave Functions, Fourier Analysis and Uncertainty—I", *Bell Syst. Tech. J.* 40.1 (1961): 43–63.

[22] Tracy, C. A. and H. Widom. "Level-Spacing Distributions and the Airy Kernel." *Commun. Math. Phys.* 159 (1994): 151-174.

[23] Trefethen, L.N. and D. Bau. *Numerical Linear Algebra.* SIAM, 1997.

[24] Xiang, S. "Asymptotics on Laguerre or Hermite polynomial expansions and their applications in Gauss quadrature." J. *Math. Anal. Appl.* 393.2 (2012): 434–444.